Confocal Microscopy and Environmental SEM Applied to Matting Water-based Lacquers

C. Patrick Royall and Athene M. Donald

Polymers and Colloids Group, Cavendish Laboratory, Department of Physics, University of Cambridge, Madingley Road, Cambridge, CB3 0HE

Two microscopy techniques are used to characterise silica matting agent in water-based lacquers. Environmental SEM permits the resolution of electron microscopy to be applied to insulating and hydrated samples in their natural state. Atomic number contrast enables silica to be readily distinguished from the polymer binder, and surface morphological information can also be obtained.

Images of optical planes within the specimen may be obtained by Confocal Laser Scanning Microscopy (CLSM). Silica is labelled with fluorescein isothiocyanate (FITC) to provide contrast against the surrounding polymer binder. By complementing the surface sensitive technique, Environmental SEM, with bulk studies using CLSM, the relationship between surface and bulk silica occupancies is studied. Maximum surface silica occupancy is reached at a concentration of 2.0% silica by weight, beyond which there is no further increase. The vertical distribution of silica is uniform throughout films of 50 μm in depth, with no tendency for surface segregation.

Introduction

Film formation in polymer latices has been extensively studied, and is at least partially understood *(1)*. The inclusion of microscopic particles of silica

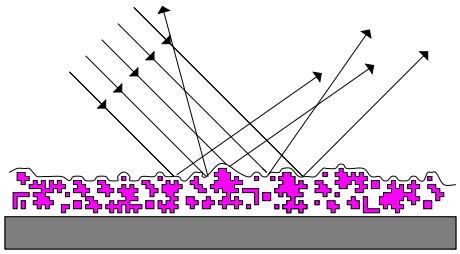

Figure 1: Light scattered by a matting coating

produces an effect known as matting, in which the intensity of specularly reflected light is reduced, figure 1 *(2)*. In this work the microstructure of a clear matting lacquer is accessed by means of two microscopy techniques, in order to understand how the addition of silica particles produces matting. Particular attention is given to the change in structure as a function of silica concentration and a simple model, based on the volume occupied by the silica in the dried lacquer film is able to account for some of the microstructural properties. It appears to go some way towards explaining how a lacquer matts at a microscopic level.

Environmental Scanning Electron Microscopy (ESEM) is a development of SEM, which brings high resolution and depth of field to samples previously inaccessible to electron microscopy. It is distinguished from conventional SEM by the presence of a partial pressure of gas inside the sample chamber *(3)*. ESEM is a surface technique like conventional SEM, and has previously been demonstrated as a unique way to image water-based latices *(4)*, *(5)*.

By elimination of out-of-focus contributions to the signal, confocal microscopy can image optical planes within a thick specimen. The transparent lacquers used are clearly well-suited to this technique. With suitable fluorescent labelling, silica particles are imaged throughout the depth of the lacquer *(6)*, *(7)*.

Image analysis enables numerical data to be extracted from micrographs. Although this process is only *semi-quantitative*, the amount of data available in every image is considerable. This quantitative data from microscopy work can be compared with the amount of silica used in the formulation.

Background

Despite its various benefits, conventional electron microscopy has been limited by the requirement for specimens to be conducting and vacuum resistant, but with ESEM almost any sample can be imaged. A differential pumping system maintains various pressure regimes inside the microscope. These are separated by what are essentially small holes which allow passage of the elec-

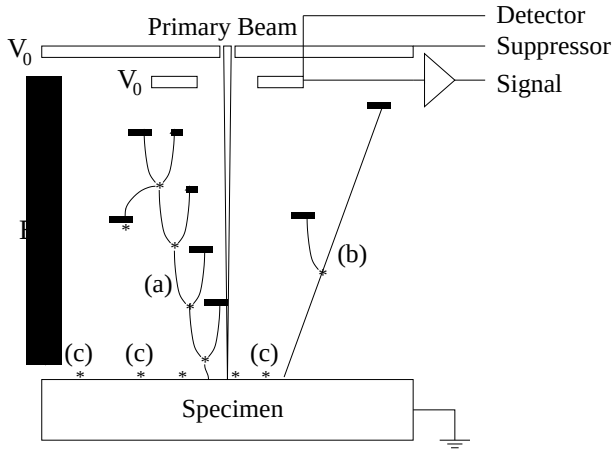

Figure 2: Signal amplification in the ESEM. Secondary electrons emitted by the sample are accelerated in an electric field, and ionise the imaging gas. Successive ionisations initiate a cascade process amplifying the signal (a). Other high-energy backscattered electrons also contribute to the signal, (b). Positive ions (marked as '') then provide charge neutralisation, (c).*

tron beam. Each section is separately pumped, maintaining a pressure gradient throughout the instrument, so the electron gun operates in a relatively high vacuum of 10^{-5} torr ($\sim 10^{-7}$ atm), whereas the sample experiences a pressure of around 5 torr (0.026 atm). At this lower pressure, enough electrons remain unscattered to produce a sharply defined probe so high-resolution images are obtained. *(3)*.

A special detector for non-vacuum operation is required. This is essentially an anode, raised to a few hundred volts, whose electric field produces a cascade from electrons emitted by the sample, figure 2. Each electron emitted from the sample produces up to 200 at the detector. The positive ions produced by this are thought to neutralise the sample surface, so insulating samples can be imaged without the need for a conducting layer *(8)*, *(9)*.

Image contrast in ESEM comes from two routes, secondary electrons and backscattered electrons. Secondary electrons are produced by ionisation events in the sample. These secondary electrons have a low energy and are accelerated by the detector field to produce the cascade (process (a) in figure 2). Secondary electrons have a rather small escape depth, of order a few nanometres. This means that more are emitted from sloping surfaces than from surfaces normal to the incident beam, since the penetration of incident beam electrons is much greater than the escape depth of secondary electrons *(10)*. So secondary electrons are sensitive to surface topography in the matting lacquers.

Backscattered electrons are incident electrons which have scattered strongly in the specimen so that they are ejected, and thus contribute to the signal, pro-

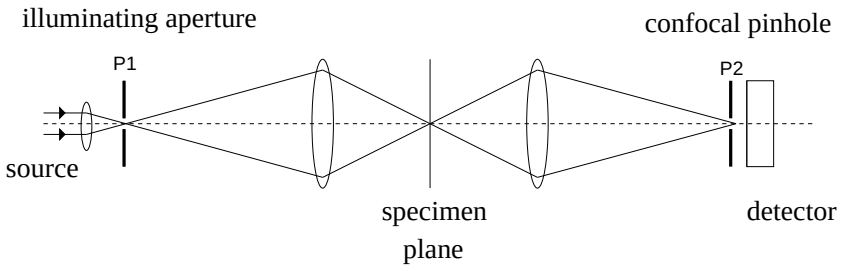

Figure 3: The principle of Confocal Microscopy. Light is focussed into a point in the sample plane by the condenser lens. The confocal pinhole rejects all light except that from the point in focus.

cess (b) in figure 2. Since backscattered electrons have a much higher energy than secondary electrons, they interact more weakly with the gas molecules and the cascade mechanism is suppressed, although the backscattered signal is still considerable *(11)*. Silicon has a higher atomic number than the surrounding polymer matrix. The incident electrons interact more strongly with the greater charge on the larger atomic nuclei, and increase the backscattered signal. So the silica particles are expected to produce bright regions, due to increased backscattering *(10)*. This means that ESEM is able to study the distribution of silica at the surface effectively, but is unable to penetrate the sample significantly.

Although confocal microscopy was originally proposed in 1957, it is only recently that the full potential of the technique has been realised. The confocal principle is shown schematically in figure 3. In conventional light microscopy, a thin planar sample is illuminated, and an image of the entire specimen is produced. This has the disadvantage that only very thin specimens may be studied (often requiring a series of slices to be made), and that out-of-focus contributions to the image degrade resolution *(6)*.

In a confocal microscope, light from only one point in the specimen passes through to the detector. All light from other regions in the sample is rejected by the confocal pinhole (figure 3). This has the advantage that, provided the sample is reasonably transparent, thick specimens may be imaged without the problem of out-of-focus contributions. In practice, in fluorescence mode, one lens may be used as both the condenser and objective, and a half-silvered mirror is used to split the incident and emitted light. This does not alter the confocal optics.

Since only a single point is observed at any one time, the specimen or light beam must be *scanned* in a similar way to a scanning electron microscope. By scanning vertically as well as horizontally, a 3d image may be produced.

The resolution is better than conventional light microscopy, at around 0.1μm in the horizontal plane, and 0.6μm in the vertical direction. As a single point is viewed at any one time, intensity is quite small. A laser source is used to improve this. Such an instrument using a laser light source is referred to as a

confocal laser scanning microscope (CLSM). Selective labelling with a fluorescent dye can enormously enhance contrast, by binding it to a region of interest in the sample. A filter is then used to allow only fluorescent light through to the detector, rejecting reflected light *(6)*. In order to study matting water-based lacquers, it is therefore necessary to label the silica matting agent with a fluorescent dye. Refractive index matching of the polymer binder with the silica matting agent allows light to penetrate up to 50 μm below the sample surface without significant attenuation.

Experiment

The lacquer used is a commercial product. The latex is largely polybutyl methacrylate, with a diameter of 85nm and polydispersity of around 0.05, measured by static light scattering. A number of additives are also used, as shown in the recipe in table 2. The ingredients are added in succession to a Cowles head rotating at 1500rpm. The speed is increased to 3000 rpm following addition of the silica, which is pre-dispersed in an aqueous solution of the fluorescent dye. The silica matting agent is based on a fumed silica, with the appearance of agglomeration. For silica characteristics, see table 1.

For confocal work the silica is labelled with a fluorescent dye, rhodamine 6G, obtained from Sigma. The dye is in the form of a chloride salt and dissolves in water to a concentration of around 0.01 mol. Rhodamine 6G is cationic, and is expected to adsorb onto the negatively charged silica surfaces, when silica is dispersed in solution prior to inclusion in the lacquer formulation *(13)*. This expectation appears to be supported by centrifuge studies, where the dye remains adsorbed onto the silica after six washes in water at 10,000 rpm for 5 minutes. Although there is some leaching out of the dye into the supernatant, the silica remains dyed red. The amount of dye required to label the silica was determined by measuring the relative brightness of the silica particles in

Table 1: Characteristics of fumed silica used in this work.

Bulk density	$0.045 g cm^{-3}$ [a]
True density	$2.2 g cm^{-3}$ [b]
Surface area	$180 m^2 g^{-1}$ [c]
Pore volume	$0.951 cm^3 g^{-1}$ [c]
Mean particle size	$4 \mu m$ [b]
Oil Absorption	$360g/100g$ of silica [b]

[a] determined in this work, [b] *(12)*, [c] determined by Crosfield R&D Group with Mercury Porosimetry.

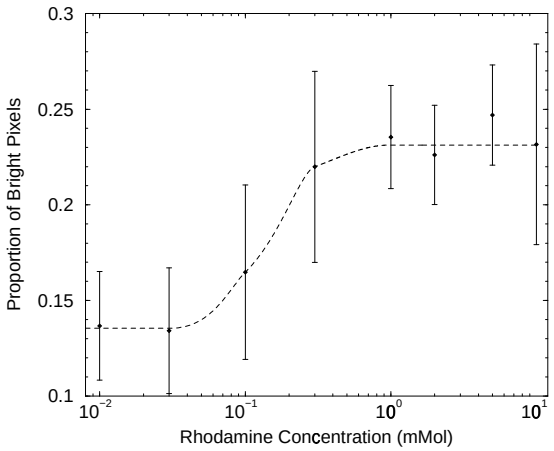

Figure 4: Image contrast is found to increase with greater rhodamine concentration up to a value of 3×10^{-4} *mol. Beyond this, the silica is assumed to be sufficiently labelled that it can all be seen.*

the images produced for various concentrations of rhodamine, holding the silica quantity constant.

The images were analysed such that bright pixels were selected corresponding to silica, and noise eliminated by requiring that the size of a bright region exceeded ten pixels. With insufficient rhodamine, there was little fluorescent signal, and not all the silica was labelled, so fewer bright pixels were observed. When enough rhodamine had been incorporated, all the silica was labelled, and the proportion of bright pixels reaches a maximum at a rhodamine concentration of 3×10^{-4} mol, figure 4. Experiments have been carried out with a 2×10^{-3} mol solution of rhodamine 6G.

Samples were produced as wet films of nominal thickness 100 μm on glass for confocal work or chromated aluminium for ESEM, with a small (20 mm) bar coater. No difference has so far been found between the substrates, as the CLSM can image samples prepared on chromated aluminium as well. These films were then dried in a dessicator with phosphorous pentoxide dessicant for 24 hours before each experiment. A helium-neon laser at 543 nm is used to excite the rhodamine, whose absorption peak is around 525 nm. A bandpass filter of 560-615 nm eliminates light that is simply reflected, but the emission peak of rhodamine 6G is sufficiently close to this range, at 555 nm that a sufficiently strong signal is produced *(14)*.

Table 2: Formulation recipe and suppliers. The silica is dispersed in the rhodamine solution prior to mixing.

Component	*Function*	*Supplier*	*% by weight*	*Density* (gcm^{-3})
Glascol C47	Latex Binder	Allied Colloids (UK)	71.4	1.04
Rhodamine 6G Soln.	Fluorescent dye	Sigma	16.8	1.0
Tegofoamex 1488	Defoamer	Tego Chemie (UK)	0.1	
TS100	Matting Agent	Degussa	0-4.0	0.045
Dowanol PnB	Coalescing aid	Dow Chemical Co.	3.81	0.9
Dowanol DPnB	Coalescing aid	Dow Chemical Co.	1.90	0.922
Tegofoamex 1488	Defoamer	Tego Chemie (UK)	0.05	1.0
Troysol LAC	Anti Cratering Agent	Troy Chemical	0.5	1.04-1.07
Glaswax E1	Surface enhancer	Allied Colloids (UK)	2.14	0.995
DSX 1514	Rheology Modifier	Henkel	0.8	1.068

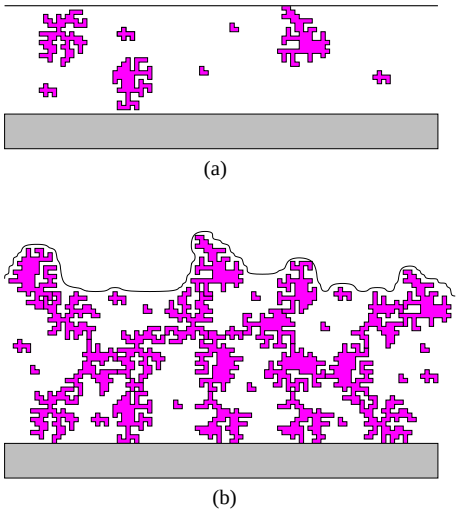

Figure 5: A schematic side-view of the dried film. Small amounts of silica are isolated in the dried film (a) but a sufficiently high concentration can produce a continuous silica structure, producing a roughened surface (b).

Silica Behaviour

Fumed silica is formed by a gas phase reaction at elevated temperature and comprises small (~20 nm) *ultimate* particles of high purity *(13)*. These are formed into larger *primary* particles in the micron range which are studied in this work. These primary particles are weakly bound *(15)* and highly porous (table 1) with an extremely low bulk density. To find the bulk density, the silica volume was found by filling a $25cm^3$ measuring cylinder, which was then allowed to fall repeatedly through $1cm$ onto a hard surface to encourage settling. This gave a value of 0.045 gcm^{-3} for the bulk dry powder.

The bulk volume occupied by such a low density material is largely air, which is present both in the pores within the particles and in the spaces between the particles. Air in pores and between particles is assumed to be replaced by polymeric material from the latex in the dried lacquer. At the silica concentrations used, table 3, this bulk volume occupied by the silica is a significant proportion of, or may even exceed that of the dried polymer film. Two scenarios are considered, figure 5. In the first case the silica is present in quite small quantities, and the dried lacquer may be regarded as a continuous layer of polymer, in which *isolated* silica particles are embedded figure 5 (a).

At a certain concentration, the silica particles touch, and can rest against one another, figure 5 (b). At this point, the structure formed by the silica is assumed to be the same as the dry powder, and thus to have the same *packing fraction*. So rather than a polymer film with isolated silica particles, we expect

a continuous silica structure, similar to the dry powder, but with spaces in between silica particles and pores now occupied by polymer. This structure may be accessed with the microscopy techniques previously described. Varying the amount of silica in the lacquer, the critical concentration required to form a silica structure may be found, by comparing the observed structure with that proposed in figure 5.

A mathematical treatment of the above description is now given. The dry mass of the lacquer is given by

$$m_{dry} = m_{wet} C_{sol} \tag{1}$$

where m_{dry} and m_{wet} are the dry and wet masses of the lacquer, $C_{sol} = 0.35$ is the solids weight fraction of the lacquer, the weight fraction of the lacquer which does not evaporate *(16)*. Since the densities of the lacquer and its components are similar (excluding the silica), table 3,

$$V_{dry} = V_{wet} C_{sol} \tag{2}$$

where V_{dry} and V_{wet} are the dry and wet volumes of the lacquer. The bulk density of dry silica is given as

$$\rho_{sil} = \frac{m_{sil}}{V_{bulk}} \tag{3}$$

where the bulk volume V_{bulk} is the volume occupied by the silica particles *and* the air between them, m_{sil} is the silica mass and ρ_{sil} the bulk density of the silica powder (0.045 gcm^{-3}). Now if the way the silica packs in the dried lacquer is the same as the powder, we expect a packing fraction p_f, which will give the proportion of volume occupied by the silica

$$V_{bulk} p_f = V_{sil} = \frac{m_{sil}}{\rho_{sil}} p_f \tag{4}$$

with V_{sil} the volume of the silica particles and their internal pores only. Assuming that the density measured for the dry powder is valid for the dried lacquer, a continuous silica structure will span the dry lacquer when

$$V_{bulk} = V_{dry} \tag{5}$$

$$\Rightarrow V_{sil} = V_{dry} p_f . \tag{6}$$

Table 3: Silica concentration and $\frac{m_{sil}}{m_0}$ as calculated from equation 9

Silica concentration (% by weight) $\frac{m_{sil}}{m_{wet}} \times 100$	$\frac{m_{sil}}{m_0}$
0	0
0.25	0.16
0.5	0.32
1.0	0.64
1.5	0.96
2.0	1.27
2.5	1.59
3.0	1.91
3.5	2.22
4.0	2.54

This is satisfied at a *critical mass*, m_0 of silica, given by

$$V_{sil} = \frac{m_0}{\rho_{sil}} p_f = V_{wet} C_{sol} p_f \tag{7}$$

$$\Rightarrow m_0 = \rho_{sil} V_{wet} C_{sol} = \frac{\rho_{sil} m_{wet} C_{sol}}{\rho_{wet}} \tag{8}$$

where ρ_{wet} is the density of the wet lacquer (≈ 1 gcm^{-3}). For a given weight fraction of silica, a parameter $\frac{m_{sil}}{m_0}$ can be assigned, such that $\frac{m_{sil}}{m_0} = 1$ when $V_{bulk} = V_{dry}$.

$$\frac{m_{sil}}{m_0} = \frac{m_{sil}}{m_{wet}} \frac{\rho_{wet}}{\rho_{sil} C_{sol}}. \tag{9}$$

where $\frac{m_{sil}}{m_{wet}}$ is the silica mass fraction of the wet lacquer. Values of $\frac{m_{sil}}{m_0}$ are given for various silica concentrations in table 3.

From equations 2, 4 and 9, we can relate $\frac{m_{sil}}{m_0}$ to the volume fraction of silica. This is equal to the fraction of silica expected in two-dimensional micrographs, assuming that the silica is uniformly distributed.

$$\frac{V_{sil}}{V_{dry}} = \frac{m_{sil}}{m_0} p_f = \phi_{sil} \tag{10}$$

where ϕ_{sil} is termed the silica occupancy. So the occupancy is linear in $\frac{m_{sil}}{m_0}$, and is equal to p_f when a continuous silica structure is formed.

Results and Analysis

This section deals with images produced from CLSM and ESEM. Image analysis is then discussed in some detail before numerical results are presented.

The contrast in the ESEM images in figure 6 agrees with expectation. Silica is distinguished as small, white regions around a few μm in size. Figure 6 *(b)* in particular suggests a degree of topographic contrast. There is considerably more silica present in figure 6 *(b)* ($\frac{m_{sil}}{m_0} = 0.95$) than figure 6 *(a)*. ($\frac{m_{sil}}{m_0} = 0.64$). There is little further increase in *surface* silica occupancy in figure 6 *(c)* ($\frac{m_{sil}}{m_0} = 1.91$) compared to the previous image, although the topology appears somewhat different. These images are in agreement with the model discussed above, although they do not conclusively demonstrate it.

Confocal images also reveal silica particles. The images shown in figure 7 are taken around the middle of the dried lacquer and are x-y scans, z being depth. The silica is easily seen from the rhodamine labelling, and the surrounding polymer has a degree of brightness as well. This is presumably the result of some rhodamine leaching out from the silica. The brightness of the polymer matrix reveals some dark regions, such as the one marked as *(i)* in figure 7 *(d)*. These are thought to be air voids.

The silica occupancy increases markedly from figure 7 *(a)* to *(c)*. Figure 7 *(a)* ($\frac{m_{sil}}{m_0} = 0.32$) appears to be in the regime of figure 5 *(a)*, of silica particles isolated in a continuous polymer medium. The same is true of figure 7 *(b)* ($\frac{m_{sil}}{m_0} = 0.64$). This is expected as the $\frac{m_{sil}}{m_0}$ values are less than 1 for both of these images. Increasing the silica concentration further might be expected to produce a continuous silica structure, but since the images are two dimensional and any structure is expected to be three dimensional, the absence of a spanning structure from figure 7 *(c)* and *(d)* ($\frac{m_{sil}}{m_0} = 1.27$ and 1.91 respectively) is not surprising. However there is no apparent increase in silica between figure 7 *(c)* and *(d)*. Like the ESEM images, the increase in silica occupancy with $\frac{m_{sil}}{m_0}$ ceases when $\frac{m_{sil}}{m_0} \gtrapprox 1$.

To go further, it is necessary to extract quantitative information from the images, and indeed to test equation 10, which predicts that at a concentration of $\frac{m_{sil}}{m_0} \approx 1$, the volume of silica is related to the volume of the dry lacquer by the packing fraction. Since a two-dimensional image of the sample is also expected to have a silica occupancy of ϕ_{sil} on average, image analysis may be used to find the silica occupancy.

The brightness of an image may be thought of as a two-dimensional function of position, $I(x, y)$. Noise may be reduced with a Gaussian blur filter *(17)*. Silica particles cause local brightness variation, as the value of $I(x, y)$ changes from a low value (darker, surrounding polymer) to a higher value (brighter silica).

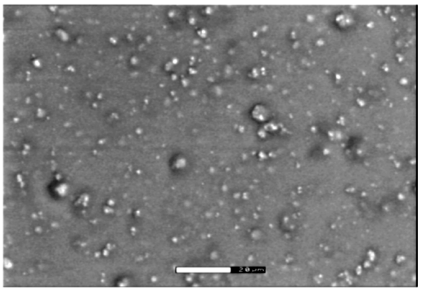

(a)

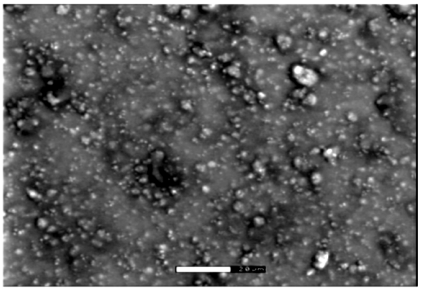

(b)

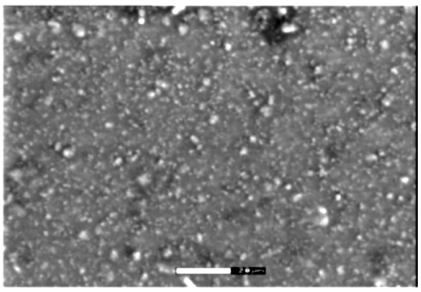

(c)

Figure 6: ESEM images of increasing silica concentration, $\frac{m_{sil}}{m_0} = 0.64$ (a), $\frac{m_{sil}}{m_0} = 1.27$ (b), $\frac{m_{sil}}{m_0} = 1.91$ (c), *bars* $= 20\mu m$.

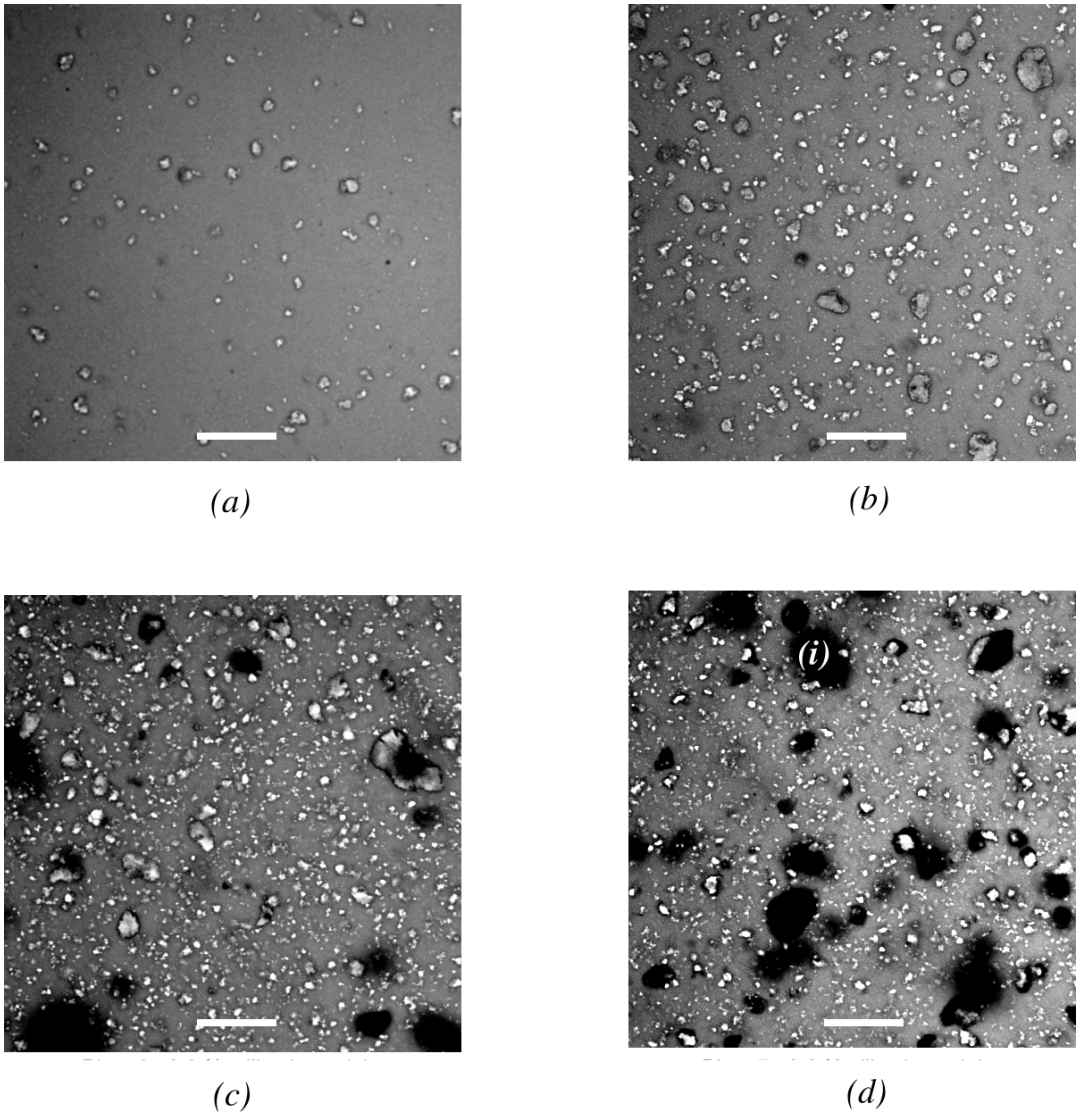

Figure 7: Confocal images of increasing silica concentration, $\frac{m_{sil}}{m_0} = 0.32$ (a), $\frac{m_{sil}}{m_0} = 0.64$ (b), $\frac{m_{sil}}{m_0} = 1.27$ (c), $\frac{m_{sil}}{m_0} = 1.91$ (d), *bars* $= 20\mu m$*, all images were taken around 10* μm *from the substrate*

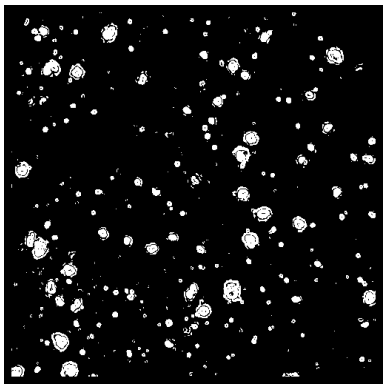

Figure 8: A binary image from figure 7 (a). *The regions in white are taken to be silica, those in black are identified as polymer. The fraction of white pixels is the silica occupancy.*

So the gradient of $I(x,y)$ increases in the vicinity of silica particles. This is found numerically by differentiating with respect to x and y, and squaring the differentials to obtain a positive value. A square root is then taken, in an algorithm known as the Sobel operator *(17)*

$$SOBEL(x,y) = \sqrt{\left(\frac{\partial}{\partial x}I(x,y)\right)^2 + \left(\frac{\partial}{\partial y}I(x,y)\right)^2}. \tag{11}$$

The resulting function, $SOBEL(x,y)$ has peaks in regions of high brightness variation, such as the edges of particles, regardless of the original brightness. Since there is intensity variation within the silica particles, which are in any case quite small, $SOBEL(x,y)$ is greater than zero in the centres of particles as well.

However the polymer background value is close to zero, as there is very little brightness variation there. If the small brightness variation from noise can be excluded by a suitably chosen *threshold*, all other brightness variation may be considered as silica. Such a thresholded image is separated into 'not silica' and 'silica', and this two-level image is termed a binary image, figure 8. The silica occupancy may then be found by dividing the number of white pixels by the total number of pixels.

The choice of threshold is found by using a sample without any silica, as this should be comprised purely from the polymer background. The threshold

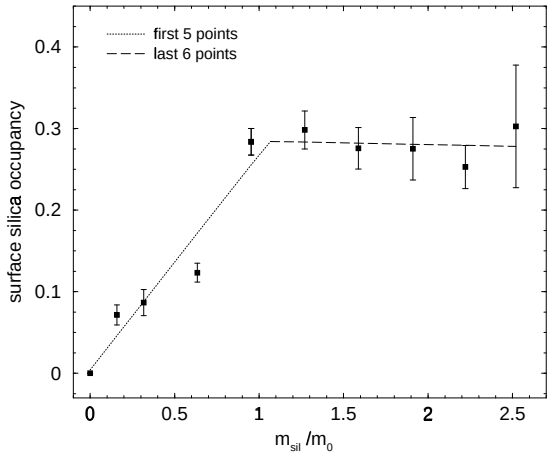

Figure 9: Surface silica occupancy as a function of $\frac{m_{sil}}{m_0}$ for ESEM images. The increase to $\frac{m_{sil}}{m_0} = 1$ and subsequent plateau are clearly seen.

is then set such that brightness variation in this image is ignored. The silica occupancy is then found for each image, and the results are plotted in figures 9 and 10 for ESEM and confocal images respectively. In the ESEM case, the surface silica occupancy is found, whereas confocal image analysis reveals the bulk silica occupancy from below the surface of the lacquer, equal to ϕ_{sil} in equation 10.

The trend is the same as that in figures 6 and 7, in that silica occupancy increases up to $\frac{m_{sil}}{m_0} \approx 1$, and then levels off. The silica occupancy of the plateau is different between the ESEM and confocal plots (figures 9 and 10), but these numbers have been arrived at via two different techniques. Apart from the two different contrast mechanisms between confocal microscopy and ESEM, confocal images contain contributions from a region around $0.6\mu m$ in depth (the z-resolution), which may contain more silica that a true plane. Alternatively, there may be a difference between the surface and the bulk. Surface tension during drying may result in a thin layer of polymer covering the silica particles, figure 5. This may reduce the amount of silica detected by ESEM.

The point for surface silica occupancy at $\frac{m_{sil}}{m_0} = 0.64$ lies some way from the best fit line, figure 9. This may be the result of a different surface occupancy regime, before a 'jump' at $\frac{m_{sil}}{m_0} \approx 1$, when the surface occupancy increases significantly. More data are required to elucidate this point further. For the present, the first five points are assumed to lie on a straight line, along with the last six. The point at $\frac{m_{sil}}{m_0} = 0.95$ is taken to lie on both lines. Regression fits to these lines are shown in figure 9. As can be seen, the data for $\frac{m_{sil}}{m_0} \lesssim 1$ agree well with a linear oncrease in surface silica with silica concentration. In addition, for $\frac{m_{sil}}{m_0} \gtrsim 1$ the regression fit is almost flat, suggesting that the maximum silica surface occupancy has been reached. The intercept was determined as

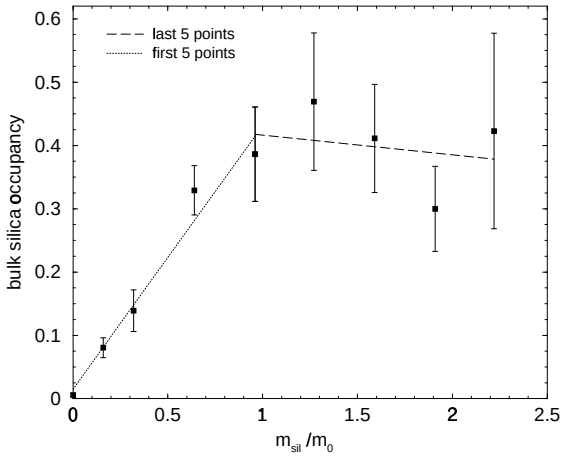

Figure 10: Bulk silica occupancy as a function of $\frac{m_{sil}}{m_0}$, from confocal images. The rise to $\frac{m_{sil}}{m_0} = 1$ appears to lie on a straight line, and the plateau for greater values is also present. The straight line and plateau region have had best fit lines applied to them.

$\frac{m_{sil}}{m_0} = 1.07 \pm 0.14$, for a silica surface occupancy of 0.281 ± 0.014. These results are in agreement with the model described above, although they do not conclusively confirm it.

Up to a value of $\frac{m_{sil}}{m_0} \approx 1$, the confocal data (figure 10) appears to follow equation 10, so we can determine the value of the packing fraction as $p_f = 0.43 \pm 0.02$ from a regression fit of the first five points. Like the ESEM data for $\frac{m_{sil}}{m_0} \gtrapprox 1$, the last five points in figure 10 show no further increase in silica occupancy. The value for the packing fraction is much less than close-packed systems (0.74 for close-packed spheres *(18)*) and in fact lies closer to that for *percolating* systems. From percolation theory, if sites on a cubic lattice are randomly filled a spanning structure is formed when a proportion of around 0.312 sites are occupied *(19)*. Taking into account the fact that the silica particles have a distribution of sizes, the higher value obtained for p_f is not unreasonable. Since the silica particles are extremely polydisperse, the smaller particles may lie between the larger ones, increasing the packing fraction as well, figure 5 (b). Effects such as gravity and surface tension in the drying lacquer are also expected to increase the packing fraction.

The plots in figures 9 and 10 support the observation from the images that the silica occupancy does not increase beyond $\frac{m_{sil}}{m_0} \approx 1$. This is at odds with equation 10, which predicts a linear increase in silica occupancy as a function of $\frac{m_{sil}}{m_0}$.

There seem to be two possibilities when $\frac{m_{sil}}{m_0} > 1$. First, if the silica structure is rigid, then it should determine the thickness of the dried film. So the film thickness should increase with $\frac{m_{sil}}{m_0}$, for $\frac{m_{sil}}{m_0} > 1$. This is not found to be the

case, as all the dried films are around the same thickness, of $20 - 30\mu m$, with no dependence on $\frac{m_{sil}}{m_0}$, the thickness being found as a by product of confocal microscopy.

Secondly, the silica structure may be crushed by the volume reduction in the drying lacquer. In this case the surface appearance of such a crushed structure may be unaltered by the precise quantity of silica present, so ESEM images will not be sensitive to $\frac{m_{sil}}{m_0}$. Below the lacquer surface, the fragments from crushed silica particles may be extremely small, since the ultimate particles are only $20nm$ in size. This is far below the maximum resolution of the confocal microscope of $0.1\mu m$, so no further increase in silica occupancy is expected for $\frac{m_{sil}}{m_0} > 1$.

Conclusions

A simple model based on volume occupied by silica in matting lacquer is able to predict microstructural properties. Both surface and bulk images and numerical image analysis suggest that at a critical silica concentration, a three dimensional silica structure is formed throughout the dried lacquer. The critical concentration required to form this structure may be predicted by measurement of the bulk density of the dry powder, assuming that the way the silica packs in the dry powder remains unchanged in the dried lacquer film.

Although it is unlikely to fully explain the behaviour of silica in matting lacquers, this simple model demonstrates the applicability of microscopy to such systems.

Acknowledgements

This work was supported by EPSRC and Crosfield Group Ltd, Warrington UK. The Authors would like to thank Dr Ian Hopkinson and Matthew Myatt for all the help with the confocal microscope, Dr Gemma Morea-Swift at Crosfields, and the suppliers of the various ingredients for the formulation.

Literature Cited

1. Keddie, J.L. *Materials Science and Engineering R-Reports*,**1997**, *21*, no 3, pp 101-170.
2. Schneider, H. *Surface Coatings International*, **1994**, *77*, no 9, p376.
3. Danilatos, G.D. *Microscopy Research and Technique*, **1993**, *25*, pp 354-361.
4. Keddie, J.L.; Meredith, P.; Jones, R.A.L.; Donald, A.M.; *Macromolecules*, **1995**, *28* , pp 2673-2682.
5. Keddie, J.L.; Meredith, P.; Jones, R.A.L.; Donald, A.M. In *Film Formation in Waterborne Coatings*; Editors, T. Provder, M. A. Winnik, M.W. Urban; ACS Symposium Series 648; American Chemical Society, 1996, Vol 648, pp 332-348.
6. Sheppard, C.J.R.; Shotton, D.M. *Confocal Laser Scanning Microscopy*, Microscopy Handbooks 38, BIOS Scientific Publishers, Oxford, England, 1997.
7. *Handbook of Biological Confocal Microscopy*, Editor Pawley, J.B.,2nd ed, Plenum Press, New York and London, 1995.
8. Fletcher, A.L. ; Thiel, B.L.; Donald, A.M.; *J. Phys D; Appl. Phys*, **1997**, *30*, pp 2249-2257.
9. Thiel, B.L.; Bache, I.C.; Fletcher, A.L.; Meredith, P.; Donald, A.M.; *J. Microscopy*, **1997**, *187*, Pt 3, pp 143-157
10. Goldstein, J.I.; Newbury, D.E.; Echlin, P.; Joy, D.C.; Romig, A.D. Jr; Lyman, C.E.; Fiori, C.; Lifshin, E. *Scanning Electron Microscopy and X-ray Microanalysis*, 2nd Edition, Plenum Press, New York, 1992.
11. Fletcher, A.L. PhD Thesis, University of Cambridge, Cambridge, England, 1997.
12. Ash, I; Ash, M *Handbook of Paint and Coating Additives*, Gower Publishing Ltd, Aldershot, England, 1996, Vol 1: Raw Materials.
13. Ihler, R.K. *The Chemistry of Silica*, Wiley, New york, 1979.
14. Haughland, R.P. *Handbook of Fluorescent Probes and Research Chemicals*, 6th ed, Molecular Probes Inc., Eugene, OR, 1996.
15. Kleinschmidt, P. *Speciality Inorganic Chemicals*, Royal Society of Chemistry Special Publication no 40, 1981, Vol: 40.
16. Turner, G.P.A. *Introduction to Paint Chemistry*, 3rd ed, Chapman and Hall, London, 1991.
17. Russ, J.C. *The Image Processing Handbook*, 2nd ed, CRC Press, Boca Raton, FL, 1995.
18. Blakemore, J.S. *Solid State Physics*, 2nd ed, Cambridge University Press, Cambridge, England, 1985.
19. Stauffer, D.; Aharony, A, *Introduction to Percolation Theory*, 2nd ed, Taylor and Francis, London, 1991.

List of Figures